Journal of Sound and Vibration 329 (2010) 4212–4226

Contents lists available at ScienceDirect

Journal of Sound and Vibration

journal homepage: www.elsevier.com/locate/jsvi

Multiple support excitations of open-plane frames by a filtered white noise and soil–structure interaction

Mehter M. Allam *

Department of Civil Engineering, Indian Institute of Science, Bangalore 560 012, India

ARTICLE INFO

Article history:
Received 2 August 2007
Received in revised form
2 January 2010
Accepted 15 April 2010
Handling Editor: L.G. Tham

ABSTRACT

Seismic structural design is essentially the estimation of structural response to a forced motion, which may be deterministic or stochastic, imposed on the ground. The assumption that the same ground motion acts at every point of the base of the structure (or at every support) is not always justifiable; particularly in case of very large structures when considerable spatial variability in ground motion can exist over significant distances—example long span bridges. This variability is partly due to the delay in arrival of the excitation at different supports (which is called the wave passage effect) and due to heterogeneity in the ground medium which results in incoherency and local effects. The current study examines the influence of the wave passage effect (in terms of delay in arrival of horizontal ground excitation at different supports and neglecting transmission through the structure) on the response of a few open-plane frame building structures with soil–structure interaction. The ground acceleration has been modeled by a suitably filtered white noise. As a special case, the ground excitation at different supports has also been treated as statistically independent to model the extreme case of incoherence due to local effects and due to modifications to the ground motion resulting from wave reflections and refractions in heterogeneous soil media. The results indicate that, even for relatively short spanned building frames, wave passage effect can be significant. In the absence of soil–structure interaction, it can significantly increase the root mean square (rms) value of the shear in extreme end columns for the stiffer frames but has negligible effect on the flexible frames when total displacements are considered. It is seen that pseudo-static displacements increasingly contribute to the rms value of column shear as the time delay increases both for the stiffer and for the more flexible frames. When soil–structure interaction is considered, wave passage effect (in terms of total displacements) is significant only for low soil shear modulus, G_s, values (where soil–structure interaction significantly lowers the fundamental frequency) and for stiff frames. The contribution of pseudo-static displacement to these rms values is found to decrease with increase in G_s. In general, wave passage effect for most interactive frames is insignificant compared to the attenuating effect a decrease in G_s has on the response of the interactive structure to uniform support excitation. When the excitations at different supports are statistically independent, it is seen that for both the stiff and flexible frames, the rms value of the column shear in extreme end columns is several times larger (more for the stiffer frames) than the value corresponding to uniform base excitation with the pseudo-static displacements contributing over 99% of the rms value of column shear. Soil–structure interaction has an attenuating effect on the rms value of the column shear, the effect decreasing with increase in G_s. Here too,

* Tel.: +91 80 2293 2643; fax: +91 80 2360 0404.
E-mail address: mehter@civil.iisc.ernet.in

0022-460X/$ - see front matter
doi:10.1016/j.jsv.2010.04.016

the pseudo-static displacements contribute very largely to the column shear. The influence of the wave passage effect on the response of three 2-bay frames with and without soil–structure interaction to a recorded horizontal accelerogram is also examined.

1. Introduction

Seismic structural design is essentially the estimation of the response of the structure to a forced motion, which may be deterministic or stochastic, imposed on the ground. In most cases, even if the structure connects at several points to the ground, the assumption that the same ground motion acts at every point of the base or at every support yields acceptable results. This assumption results in the uniform support or rigid base excitation approach.

It is generally accepted that seismic ground motions can have significant spatial variation, particularly over distances associated with long span bridges. The spatial variability is attributed to three phenomena [1,2]: (1) the wave passage effect which is the difference in arrival times of seismic waves at different stations, (2) the 'incoherence effect' which is the loss of coherency in the ground motion resulting from reflections and refractions of waves in the heterogeneous medium of the ground, and (3) the local effect which is the filtering effect of local soil conditions on the frequency content and amplitude of the bed rock motion.

The study of a simplified bridge model [3] subjected to a traveling disturbance consisting of packets of damped oscillatory waves with random amplitudes, frequencies, arrival times, phases and velocities of propagation indicated that a finite transmission time for a seismic disturbance can significantly reduce the probability of survival of the structure.

It has been reported by Kiureghian and Neuenhofer [1] that the cross-correlation coefficient between ground displacement at one station and oscillator response at another station very rapidly diminishes from unity with increase in the oscillator frequency for ground acceleration represented by a white noise passed through the twin filters of the Kanai–Tajimi model described by Clough and Penzien [4]. The study does not account for soil–structure interaction at the multiple supports and the results of an example application on a two-span continuous beam (both spans of 50 m) show that totally uncorrelated support excitations could result in mid-span deflections exceeding those corresponding to the case of totally correlated support excitations.

Except for structures founded on hard rock, the phenomenon of soil–structure interaction significantly affects structural response to static and dynamics loads. It has been well established in the literature [5–7] that reduction in the natural frequencies of the system occurs when foundation flexibility is introduced in the non-interactive system. In particular, for open-plane frames on isolated foundations, soil–structure interaction lowers the fundamental frequency—the reduction being severe for softer soils (lower soil shear modulus, G_s, values), stiffer superstructures and smaller footing sizes. It also modifies the mode shapes [8,9]. It has been determined that the fundamental mode shape almost entirely determines the response of both non-interactive as well as structures with soil–structure interaction to seismic excitations [8]. It has also been reported that when the seismic excitation is represented by a fully coherent white noise acting at all the supports, soil–structure interaction is always beneficial in case of realistically proportioned superstructure frames on isolated footings [9].

The existing literature offers limited information on the response of open-plane frames on isolated footing to multiple support excitations. Compared to bridge spans, in such structures the spacing of footings is small and the soil characteristics under different footings are not likely to vary significantly. Consequently, wave passage effects may be more important than incoherency in the ground motion at different supports arising from differing soil conditions at the supports (local effect) and the 'incoherency effect.' A recent study [10] on the response of a single open-plane frame subjected to five seismic acceleration records indicated that a multiple support excitations approach (which accounts for wave passage effect) yields significantly different peak column shears from those obtained by a uniform support approach in the absence of soil–structure interaction. The pseudo-static contribution to the peak response was significant for some excitations. When soil–structure interaction is considered, wave passage effect yielded larger peak column shears for many of the excitations over a large range of shear modulus of soil. The pseudo-static contribution could be significant even for the frame founded on hard soil.

Some studies involving multiple support excitations use random processes with defined power spectral densities to model the ground motion at different stations and these compare very well with the actual earthquake data at similar sites [11]. Since the fundamental frequency almost completely determines the structure response to support excitation (whether totally correlated, or with some degree of incoherency at different supports), the use of such random processes may not yield a comprehensive picture if the fundamental frequency of the system under investigation lies outside the effective range of the power spectral density function of the random process. While it is well known that soil–structure interaction decreases the fundamental frequency of the superstructure and also modifies the fundamental mode shape, literature is scarce on what effect soil–structure interaction has on the response to multiple support excitations. A more general picture of effect of multiple support excitations can be obtained if a white noise, which specifies equal power in all frequencies, models the ground excitation. While this also eliminates unintended cases of resonance that may occur for some combinations of soil and structure parameters when an artificial strong ground motion is used, a difficulty arises in

the case of multiple support excitations. As will be discussed subsequently, when white noise models the ground acceleration, the evaluation of the response deals with integrands containing cross-spectral density functions both between displacements at different supports and also between accelerations and displacements between supports. These integrands possess higher order singularities or poles at the origin of the frequency axis. The lack of a solution for this condition can be countered by passing the white noise though a filter of the Kania–Tajimi type [4]. These results, for a proper choice of filter parameters, in the spectral density function of the ground acceleration being zero at the origin and very flat over a wide range of frequency.

In this paper the influence of wave passage effect (in terms of delay in arrival of horizontal ground excitation at different supports and neglecting transmission through the structure) on the response of an open-plane frame with soil–structure interaction is studied using a suitably filtered white noise to model the ground acceleration. For complete understanding of the phenomena, the specific case of ground acceleration at different supports being statistically independent is also examined which will thus be representative of the extreme case of incoherence due to the "local effect" and the "incoherence effect" resulting from wave reflections and refractions in heterogeneous soil media. The influence of wave passage effect on the response of three 2-bay frames with and without soil–structure interaction to a recorded horizontal accelerogram (the NS component of the El Centro 1940 earthquake) is also examined.

2. Equations of motion for a structure subjected to multiple support excitations with soil–structure interaction

For the open-plane frame on isolated footings shown in Fig. 1(a), the equations of motion for the n-degree-of-freedom system subjected to m support excitations can be expressed as

$$\begin{bmatrix} \mathbf{m}_s & \mathbf{m}_{sf} \\ \mathbf{m}_{fs} & \mathbf{m}_f \end{bmatrix} \begin{Bmatrix} \ddot{\mathbf{v}}_s^t \\ \ddot{\mathbf{v}}_f^t \end{Bmatrix} + \begin{bmatrix} \mathbf{c}_s & \mathbf{c}_{sf} \\ \mathbf{c}_{fs} & \mathbf{c}_f \end{bmatrix} \begin{Bmatrix} \dot{\mathbf{v}}_s^t \\ \dot{\mathbf{v}}_f^t \end{Bmatrix} + \begin{bmatrix} \mathbf{k}_s & \mathbf{k}_{sf} \\ \mathbf{k}_{fs} & \mathbf{k}_f \end{bmatrix} \begin{Bmatrix} \mathbf{v}_s^t \\ \mathbf{v}_f^t \end{Bmatrix} = \begin{Bmatrix} \mathbf{0} \\ \mathbf{R}^t \end{Bmatrix} \tag{1}$$

by treating the open-plane frame with footings as Substructure 1 and the half-space of soil below as Substructure 2 (Fig. 1(b)). The suffixes s and f refer to degrees of freedom pertaining to nodes in the superstructure and in the foundation, respectively. The suffixes sf and fs refer to degrees of freedom pertaining to nodes common to superstructure and foundation elements. The total displacement vector $\{\mathbf{v}^t\}$ can be separated into a vector of displacements induced by the

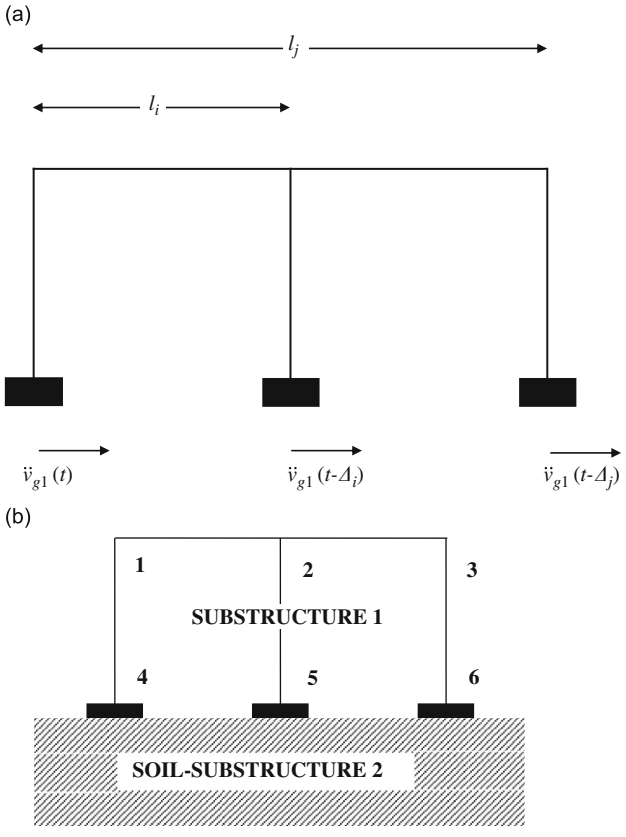

Fig. 1. Open-plane frame subjected to multiple support excitations.

dynamic forces $\{\mathbf{v}^d\}$ and that by the ground motion $\{\mathbf{v}^p\}$

$$\begin{Bmatrix} \mathbf{v}_s^t \\ \mathbf{v}_f^t \end{Bmatrix} = \begin{Bmatrix} \mathbf{v}_s^d \\ \mathbf{v}_f^d \end{Bmatrix} + \begin{Bmatrix} \mathbf{v}_s^p \\ \mathbf{v}_g \end{Bmatrix} \tag{2}$$

For the non-interactive system, $\{\mathbf{v}_f^d\} = \{\mathbf{0}\}$ since dynamic base displacements are not permitted. The vector $\{\mathbf{v}^p\}$ of displacements induced by the ground motion can be represented as $\{\mathbf{v}^p\}^{\mathrm{T}} = [\,\mathbf{v}_s^{p\mathrm{T}} \quad \mathbf{v}_g^{\mathrm{T}}\,]^{\mathrm{T}}$, where the vector $\{\mathbf{v}_g\}$ represents the displacements imposed on the degrees of freedom associated with the supports. In the current study, these would consist of horizontal displacements imposed at the support nodes with zero displacements in the vertical and rotational degrees of freedom associated with the supports. The vector $\{\mathbf{R}^t\}$ of forces on the foundation nodes can be separated in to components

$$\{\mathbf{R}^t\} = \{\mathbf{R}^d\} + \{\mathbf{R}^p\} \tag{3}$$

where $\{\mathbf{R}^d\}$ are the support reactions produced by the dynamic forces and $\{\mathbf{R}^p\}$ are the support reactions produced by the motion of the supports. For rigid base excitation, the entire frame translates so that no reactions are developed at the supports, i.e. $\{\mathbf{R}^p\}=\{\mathbf{0}\}$. For non-uniform translation of the supports, the entire structure undergoes distortions, which may be called pseudo-static displacements, as a result of which support reactions are developed. That is, $\{\mathbf{R}^p\} \neq \{\mathbf{0}\}$.

Considering the equilibrium of the system subjected to a static set of support displacements, $\{\mathbf{v}_g\}$, the static equivalent of Eq. (1) yields

$$\begin{bmatrix} \mathbf{k}_s & \mathbf{k}_{sf} \\ \mathbf{k}_{fs} & \mathbf{k}_f \end{bmatrix} \begin{Bmatrix} \mathbf{v}_s^p \\ \mathbf{v}_g \end{Bmatrix} = \begin{Bmatrix} \mathbf{0} \\ \mathbf{R}^p \end{Bmatrix} \tag{4}$$

So that

$$\{\mathbf{v}_s^p\} = -[\mathbf{k}_s]^{-1}[\mathbf{k}_{sf}]\{\mathbf{v}_g\} = [\overline{\mathbf{K}}]\{\mathbf{v}_g\} \tag{5}$$

And

$$[\mathbf{k}_{fs}]\{\mathbf{v}_s^p\} + [\mathbf{k}_f]\{\mathbf{v}_g\} = \{\mathbf{R}^p\} \tag{5a}$$

where the restraint forces $\{\mathbf{R}^p\}$ must be applied to the interface between Substructures 1 and 2 to obtain the required support displacements $\{\mathbf{v}_g\}$. This equation can also be written as

$$[\mathbf{k}_{fs}]\{\mathbf{v}_s^p\} + [\mathbf{k}_f]\{\mathbf{v}_g\} - \{\mathbf{R}^p\} = \mathbf{0} \tag{5b}$$

Substituting Eq. (2) into Eq. (1) and transferring the load vectors arising from the pseudo-static motions to the right-hand side, the following equation is obtained:

$$\begin{aligned} &\begin{bmatrix} \mathbf{m}_s & \mathbf{m}_{sf} \\ \mathbf{m}_{fs} & \mathbf{m}_f \end{bmatrix} \begin{Bmatrix} \ddot{\mathbf{v}}_s^d \\ \ddot{\mathbf{v}}_f^d \end{Bmatrix} + \begin{bmatrix} \mathbf{c}_s & \mathbf{c}_{sf} \\ \mathbf{c}_{fs} & \mathbf{c}_f \end{bmatrix} \begin{Bmatrix} \dot{\mathbf{v}}_s^d \\ \dot{\mathbf{v}}_f^d \end{Bmatrix} + \begin{bmatrix} \mathbf{k}_s & \mathbf{k}_{sf} \\ \mathbf{k}_{fs} & \mathbf{k}_f \end{bmatrix} \begin{Bmatrix} \mathbf{v}_s^d \\ \mathbf{v}_f^d \end{Bmatrix} \\ &= -\begin{bmatrix} \mathbf{m}_s & \mathbf{m}_{sf} \\ \mathbf{m}_{fs} & \mathbf{m}_f \end{bmatrix} \begin{Bmatrix} \ddot{\mathbf{v}}_s^p \\ \ddot{\mathbf{v}}_g \end{Bmatrix} - \begin{bmatrix} \mathbf{c}_s & \mathbf{c}_{sf} \\ \mathbf{c}_{fs} & \mathbf{c}_f \end{bmatrix} \begin{Bmatrix} \dot{\mathbf{v}}_s^p \\ \dot{\mathbf{v}}_g \end{Bmatrix} - \begin{bmatrix} \mathbf{k}_s & \mathbf{k}_{sf} \\ \mathbf{k}_{fs} & \mathbf{k}_f \end{bmatrix} \begin{Bmatrix} \mathbf{v}_s^p \\ \mathbf{v}_g \end{Bmatrix} + \begin{Bmatrix} \mathbf{0} \\ \mathbf{R}^t \end{Bmatrix} \end{aligned} \tag{1a}$$

The vector on the right-hand side of Eq. (4) can be transferred to the left-hand side which then constitutes a zero vector. This zero vector can be added to the right-hand side of Eq. (1a) without affecting the force equilibrium. The resulting equation is

$$\begin{aligned} &\begin{bmatrix} \mathbf{m}_s & \mathbf{m}_{sf} \\ \mathbf{m}_{fs} & \mathbf{m}_f \end{bmatrix} \begin{Bmatrix} \ddot{\mathbf{v}}_s^d \\ \ddot{\mathbf{v}}_f^d \end{Bmatrix} + \begin{bmatrix} \mathbf{c}_s & \mathbf{c}_{sf} \\ \mathbf{c}_{fs} & \mathbf{c}_f \end{bmatrix} \begin{Bmatrix} \dot{\mathbf{v}}_s^d \\ \dot{\mathbf{v}}_f^d \end{Bmatrix} + \begin{bmatrix} \mathbf{k}_s & \mathbf{k}_{sf} \\ \mathbf{k}_{fs} & \mathbf{k}_f \end{bmatrix} \begin{Bmatrix} \mathbf{v}_s^d \\ \mathbf{v}_f^d \end{Bmatrix} \\ &= -\begin{bmatrix} \mathbf{m}_s & \mathbf{m}_{sf} \\ \mathbf{m}_{fs} & \mathbf{m}_f \end{bmatrix} \begin{Bmatrix} \ddot{\mathbf{v}}_s^p \\ \ddot{\mathbf{v}}_g \end{Bmatrix} - \begin{bmatrix} \mathbf{c}_s & \mathbf{c}_{sf} \\ \mathbf{c}_{fs} & \mathbf{c}_f \end{bmatrix} \begin{Bmatrix} \dot{\mathbf{v}}_s^p \\ \dot{\mathbf{v}}_g \end{Bmatrix} + \begin{Bmatrix} \mathbf{0} \\ \mathbf{R}^t - \mathbf{R}^p \end{Bmatrix} \end{aligned} \tag{1b}$$

$\mathbf{R}^d = \mathbf{R}^t - \mathbf{R}^p$ are the combined interface forces. When the soil impedance is modeled by a frequency-independent spring-dashpot model

$$\{\mathbf{R}^d\} = -[\mathbf{c}_{ss}]\{\dot{\mathbf{v}}_f^d\} - [\mathbf{k}_{ss}]\{\mathbf{v}_f^d\}$$

In the current study, the frequency-independent soil stiffness coefficients used by Pais and Kausel [12] have been adopted. Substituting for the combined interface forces in Eq. (1b) and rearranging terms,

$$\begin{aligned} &\begin{bmatrix} \mathbf{m}_s & \mathbf{m}_{sf} \\ \mathbf{m}_{fs} & \mathbf{m}_f \end{bmatrix} \begin{Bmatrix} \ddot{\mathbf{v}}_s^d \\ \ddot{\mathbf{v}}_f^d \end{Bmatrix} + \begin{bmatrix} \mathbf{c}_s & \mathbf{c}_{sf} \\ \mathbf{c}_{fs} & \mathbf{c}_f + \mathbf{c}_{ss} \end{bmatrix} \begin{Bmatrix} \dot{\mathbf{v}}_s^d \\ \dot{\mathbf{v}}_f^d \end{Bmatrix} + \begin{bmatrix} \mathbf{k}_s & \mathbf{k}_{sf} \\ \mathbf{k}_{fs} & \mathbf{k}_f + \mathbf{k}_{ss} \end{bmatrix} \begin{Bmatrix} \mathbf{v}_s^d \\ \mathbf{v}_f^d \end{Bmatrix} \\ &= -\begin{bmatrix} \mathbf{m}_s & \mathbf{m}_{sf} \\ \mathbf{m}_{fs} & \mathbf{m}_f \end{bmatrix} \begin{Bmatrix} \ddot{\mathbf{v}}_s^p \\ \ddot{\mathbf{v}}_g \end{Bmatrix} - \begin{bmatrix} \mathbf{c}_s & \mathbf{c}_{sf} \\ \mathbf{c}_{fs} & \mathbf{c}_f \end{bmatrix} \begin{Bmatrix} \dot{\mathbf{v}}_s^p \\ \dot{\mathbf{v}}_g \end{Bmatrix} \end{aligned} \tag{1c}$$

The damping terms on the right-hand side of Eq. (1c) generally make a lesser contribution to the effective load compared to the mass terms and are ignored in the current investigation. This simplifies Eq. (1c) in case of a lumped mass formulation which makes the **M** matrix diagonal to

$$\begin{bmatrix} \mathbf{m}_s & \\ & \mathbf{m}_f \end{bmatrix} \begin{Bmatrix} \ddot{\mathbf{v}}_s^d \\ \ddot{\mathbf{v}}_f^d \end{Bmatrix} + \begin{bmatrix} \mathbf{c}_s & \mathbf{c}_{sf} \\ \mathbf{c}_{fs} & \mathbf{c}_f + \mathbf{c}_{ss} \end{bmatrix} \begin{Bmatrix} \dot{\mathbf{v}}_s^d \\ \dot{\mathbf{v}}_f^d \end{Bmatrix} + \begin{bmatrix} \mathbf{k}_s & \mathbf{k}_{sf} \\ \mathbf{k}_{fs} & \mathbf{k}_f + \mathbf{k}_{ss} \end{bmatrix} \begin{Bmatrix} \mathbf{v}_s^d \\ \mathbf{v}_f^d \end{Bmatrix} = - \begin{bmatrix} \mathbf{m}_s & \\ & \mathbf{m}_f \end{bmatrix} \begin{Bmatrix} \ddot{\mathbf{v}}_s^p \\ \ddot{\mathbf{v}}_g \end{Bmatrix} \tag{6}$$

For the system in the absence of soil–structure interaction, the **C** matrix can be dealt with in two ways. It can be proportional to the mass and stiffness matrices. Alternatively, the $[\mathbf{c}_s]$ matrix can be generated for the superstructure after assigning values to the damping ratios of the different modes of vibration of the superstructure. In this approach, the matrices $[\mathbf{c}_{sf}]$, $[\mathbf{c}_{fs}]$ and $[\mathbf{c}_f]$ in Eq. (1) are null matrices. The second approach has been adopted in the current study for the non-interactive structure. When the second approach is applied to the case where soil–structure interaction is considered, the $[\mathbf{c}_f]$ matrix contains only elements of soil damping, i.e., $[\mathbf{c}_{ss}]$ (possibly frequency independent), while the matrices $[\mathbf{c}_{sf}]$ and $[\mathbf{c}_{fs}]$ continue to be null matrices. Such a damping matrix does not strictly satisfy orthogonality conditions but it has been reported in earlier studies [13–16] that such an assumption does not cause excessive loss of accuracy. For convenience, as has been done in the current study, it can also be assumed that frequency-independent springs represent the soil reaction and that the entire damping matrix **C** on the left-hand side of Eq. (6) is an orthogonal matrix and suitable modal damping ratios can be assumed for all the modes of vibration of the structure with soil–structure interaction. While studies in literature [13–16] indicate that this approach does have a built in error, the error can vary from 5% to 20% and, in a qualitative exercise like the current study, the convenience of uncoupling the equations of motion can justify the error of assuming normal modes of vibration.

3. Cross-spectral density functions for the multiple support excitations

If the free field horizontal seismic acceleration $\ddot{\mathbf{v}}_{g1}(\mathbf{t})$ at the outer most left support travels towards the right with a wave velocity v_s, the excitation at the ith support at a distance l_i is $\ddot{\mathbf{v}}_{gi}(\mathbf{t}) = \ddot{\mathbf{v}}_{g1}(\mathbf{t}-\boldsymbol{\Delta}_i)$, where $\Delta_i = l_i/v_s$ is the time delay for the excitation to reach the ith support. For a stationary and ergodic process, the auto-correlation function of the excitation at any support is the same as the excitation travels from left to right, while the cross-correlation function between the ith and jth supports ($i \neq j$) is

$$\begin{aligned} \mathbf{R}_{\ddot{\mathbf{v}}_{ij}}(\boldsymbol{\tau}) &= \underset{T\to\infty}{Lt} \frac{1}{T} \int_{-T/2}^{T/2} \ddot{\mathbf{v}}_{gi}(\mathbf{t}) \ddot{\mathbf{v}}_{gj}(\mathbf{t}+\boldsymbol{\tau})\, \mathrm{d}\mathbf{t} = \underset{T\to\infty}{Lt} \frac{1}{T} \int_{-T/2}^{T/2} \ddot{\mathbf{v}}_{g1}(\mathbf{t}-\boldsymbol{\Delta}_i) \ddot{\mathbf{v}}_{g1}(\mathbf{t}-\boldsymbol{\Delta}_j+\boldsymbol{\tau})\, \mathrm{d}\mathbf{t} \\ &= R_{\ddot{v}_{g1}}(\tau - \Delta_j + \Delta_i) \end{aligned} \tag{7}$$

Further, if $\mathbf{S}_{\ddot{\mathbf{v}}_{g1}}(\omega)$ is the spectral density function of the excitation at any support, the cross-spectral function of the excitation between supports i and j is

$$S_{\ddot{v}_{g_{ij}}}(\omega) = \int_{-\infty}^{\infty} R_{\ddot{v}_{g_{ij}}}(\tau) \mathrm{e}^{-\mathrm{i}\omega\tau}\, \mathrm{d}\tau$$

or

$$S_{\ddot{v}_{ij}}(\omega) = S_{\ddot{v}_{g1}} \mathrm{e}^{-\mathrm{i}\omega(\Delta_j - \Delta_i)} \tag{8}$$

When $\Delta_j - \Delta_i = 0$ then $\mathbf{S}_{\ddot{\mathbf{v}}_{g_{ij}}}(\omega) = \mathbf{S}_{\ddot{\mathbf{v}}_{g_{ji}}}(\omega)$ and when $\Delta_j - \Delta_i \neq 0$ then $\mathrm{e}^{\mathrm{i}\omega(\Delta_j - \Delta_i)}$ differs from unity and represents the degree of incoherence introduced by the wave passage effect.

The spectral density function of the ground acceleration at any support is obtained by filtering a white noise $S_{\ddot{v}_{g_1}}(\omega) = S_0$ through the Kanai–Tajimi filter to obtain

$$S_{\ddot{v}_{g1}}(\omega) = \frac{\{\omega_f^4 + 4\xi_f^2 \omega_f^2 \omega^2\} \omega^4 S_0}{\{(\omega_f^2 - \omega^2)^2 + 4\xi_f^2 \omega_f^2 \omega^2\}\{(\omega_g^2 - \omega^2)^2 + 4\xi_g^2 \omega_g^2 \omega^2\}}$$

A value for ω_g larger than unity ensures that the spectral density function is zero at the origin. Judicious choice of value for the parameters ξ_f, ξ_g, ω_f and ω_g (0.7, 0.7, 10,000 and 1.5, respectively) results in the spectral density function being practically constant in the frequency range 6–3000 rad s^{-1} as seen in Fig. 2.

4. Correlation functions for the response in terms of column shear and storey sway

If $[\boldsymbol{\phi}]$ is the matrix of eigenvectors associated with the undamped form of the equations of motion (Eq. (6)) during free vibrations and $[\boldsymbol{\omega}]$ is the corresponding diagonal matrix of natural frequencies, the dynamic nodal displacements at time t and $t+\tau$ are

$$\{\mathbf{v}(t)\} = [\boldsymbol{\phi}]\{\mathbf{q}(\mathbf{t})\} \quad \text{and} \quad \{\mathbf{v}(\mathbf{t}+\boldsymbol{\tau})\} = [\boldsymbol{\phi}]\{\mathbf{q}(\mathbf{t}+\boldsymbol{\tau})\}$$

where $\{\mathbf{q}(t)\}$ is a modal amplitude.

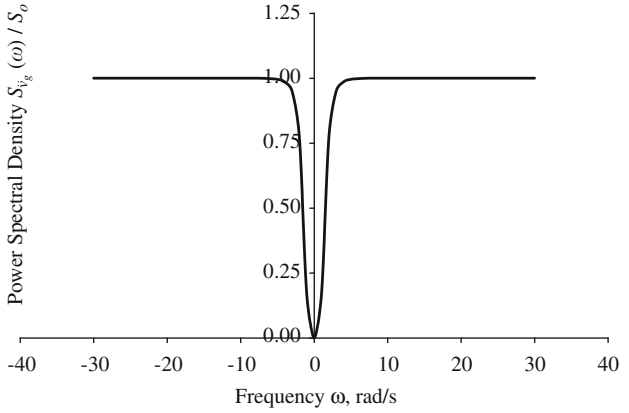

Fig. 2. Spectral density function for filtered white noise.

The nodal displacements of interest (with respect to member m_e) can be obtained from the frame nodal displacements $\{\mathbf{v}(\mathbf{t})\}$ using a selection matrix $[\mathbf{y}]_{m_e}$

$$\{\mathbf{v}(\mathbf{t})\}_{m_e} = [\mathbf{y}]_{m_e}\{\mathbf{v}(\mathbf{t})\} = [\mathbf{y}]_{m_e}[\boldsymbol{\phi}]\{\mathbf{q}(\mathbf{t})\} \tag{9}$$

The equations of motion after uncoupling are

$$\ddot{q}_r(t) + 2\xi_r\omega_r\dot{q}_r(t) + \omega_r^2 q_r(t) = p_r(t) \tag{10}$$

where ξ_r is the damping ratio associated with the rth mode of vibration (r=1, 2, 3, …, n) and

$$p_r(t) = \{\boldsymbol{\phi}_r\}^{\mathrm{T}}[\mathbf{m}]\begin{Bmatrix} \overline{\mathbf{K}}\ddot{\mathbf{v}}_g(\mathbf{t}) \\ \ddot{\mathbf{v}}_g(\mathbf{t}) \end{Bmatrix} \quad \text{or} \quad p_r(t) = \{\boldsymbol{\phi}_r\}^{\mathrm{T}}[\mathbf{m}]\begin{bmatrix} \overline{\mathbf{K}} \\ \mathbf{I} \end{bmatrix}\{\ddot{\mathbf{v}}_g(\mathbf{t})\} \tag{11}$$

is the generalized load for mode r and I is an identity matrix of size $m \times m$.

The generalized response $q_r(t)$ of a linear system in the rth mode of vibration to an arbitrary excitation $p_r(t)$ can be written in the form of the convolution integral

$$q_r(t) = \int p_r(\lambda_r)g_r(t-\lambda_r)\,\mathrm{d}\lambda_r \tag{12a}$$

where $g_r(t)$ is the impulse response.

Or, in the frequency domain

$$Q_r(\omega) = G_r(\omega)P_r(\omega) \tag{12b}$$

where $\mathbf{G}_r(\omega) = 1/(\boldsymbol{\omega}_r^2 - \boldsymbol{\omega}^2 + 2\mathrm{i}\boldsymbol{\xi}_r\boldsymbol{\omega}_r\omega)$.

The column shear, which is the generic response quantity of interest, can be expressed as

$$\mathrm{shear}_{m_e}(t) = [\mathbf{CSA}^{\mathrm{T}}]\{\mathbf{v}^t(\mathbf{t})_{m_e}\}/l_{m_e} \tag{13}$$

where l_{m_e} is the member length and $\mathrm{CSA}^{\mathrm{T}}$ is the matrix which converts the nodal *total* displacements $v^t(t)_{m_e}$ of member m_e to shear force. The auto-correlation of the column shear in member m_e is

$$R_{\mathrm{shear},m_e}(\tau) = \lim_{T\to\infty}\frac{1}{T}\int_{-T/2}^{T/2}\mathrm{shear}_{m_e}(t)\mathrm{shear}_{m_e}(t+\tau)\,\mathrm{d}t \tag{14}$$

The mean square value of the column shear can also be expressed (in a more convenient form of Eq. (14)) as

$$R_{\mathrm{shear},m_e}(0) = \tfrac{1}{l_{m_e}^2}[\mathbf{CSA}^{\mathrm{T}}][\mathbf{y}]_{m_e}[\mathbf{R}_{v^t}(\mathbf{0})][\mathbf{y}]_{m_e}^{\mathrm{T}}[\mathbf{CSA}^{\mathrm{T}}]^{\mathrm{T}} \tag{15}$$

The elements of the $\mathbf{R}_{v^t}(\mathbf{0})$ matrix in Eq. (15) are given in the Appendix for the non-interactive structure.

It is of interest to note here that evaluation of Eq. (14) or Eq. (15) requires evaluation of the residues in contour integration for various $\mathbf{S}_{\ddot{v}_{g_{ij}}}(\omega)$. When i=j and for $i>j$ the poles lying in the upper half of the complex plane are used in computing the residues. When $i<j$, while computing the residues for any combination of the modal frequencies ω_r, ω_s the exponential term $\mathrm{e}^{-\mathrm{i}\Delta\varpi}$ in the numerator of the integrand will exceed unity when the complex values of the poles in the upper half-plane are substituted. This can be avoided by reversing the limits of integration and using the poles lying in the lower half of the complex plane.

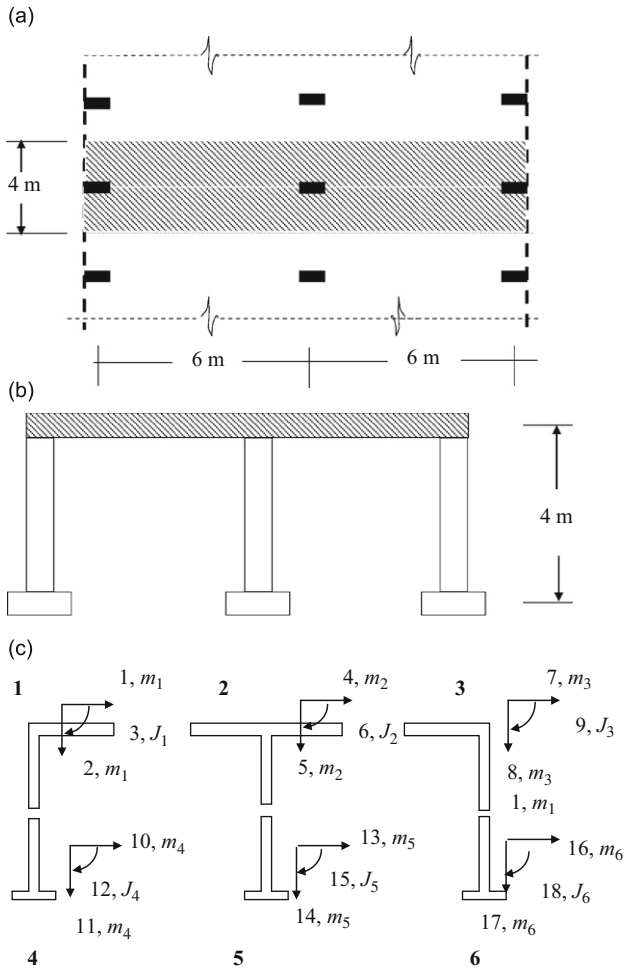

Fig. 3. Typical open-plane frame on isolated footings: (a) plan, (b) transverse section and (c) mass discretization.

5. Frames adopted and range of soil properties

Single-storey 1-bay and 2-bay frames of flat slab construction were adopted for the study. Fig. 3(a) and (b) show the plan and transverse section of the 2-bay single-storey frame. For both bay types, a bay span of 6 m was considered. The slab is 0.3 m thick (Fig. 3(b)). In the transverse section (which is also the direction of the ground motion), the slab with columns constitutes a flexible frame as shown shaded in Fig. 3(a) with an inter-frame spacing of 4 m. As seen in Fig. 3(a), the larger column cross-section direction is in the direction of the ground motion and in the plane of the frame. In each bay type, selecting the column sectional dimensions and the storey height has yielded 3 frames. Frame 1 has column section of 0.2×0.5 m and storey height of 3.0 m. Frames 2 and 3 have a common storey height of 4.0 m but column sections of 0.3×0.4 m and 0.3×0.3 m, respectively. Fig. 1(a) indicates a typical 2-bay frame idealized as an assembly of flexible members. A typical scheme for labeling the nodes is shown in Fig. 1(b). The members are assumed to undergo only flexural and axial deformations. For a plane frame, torsional deformations do not exist while shear deformations can be ignored. Each node possesses 3 degrees of freedom. The stiffness matrix of the frame is assembled using the element stiffness matrix of a prismatic member that is derived from the slope deflection method with provision made for axial deformation. Fig. 3(c) indicates the mass discretization of a 2-bay frame. The portion of the structure surrounding each node is treated as a rigid body. The corresponding masses and mass moment of inertia associated with each number node is also shown.

The material properties of structural members used for the linear elastic analysis of these frames are modulus of elasticity of concrete E_c=22 GPa and mass density of concrete ρ_c=2400 kg/m^3. The fundamental undamped frequencies of these frames (Table 1) in the absence of soil–structure interaction range between 14.85 and 41.98 rad/s.

To permit soil–structure interaction in the 1-bay and 2-bay frames adopted in the study, rigid bases of concrete of size $1.0\,\text{m} \times 0.5\,\text{m}$ and 0.3 m thick were selected and may be considered as adequate in medium to hard soils. The larger plan dimension of the footing (1.0 m) is in the direction of the ground motion.

Table 1
Undamped fundamental frequencies of the frames with soil–structure interaction.

Frame type	G_s (MPa)						
	10	50	90	150	300	500	Fixed base
	Undamped fundamental frequency						
1-Bay Frame 1	19.31	27.26	30.59	33.42	36.66	38.44	41.98
1-Bay Frame 2	13.18	18.05	19.96	21.42	22.93	23.68	25.02
1-Bay Fame 3	10.54	14.07	15.09	15.74	16.33	16.59	17.02
2-Bay Fame 1	17.75	24.19	27.05	29.51	32.35	33.92	37.07
2-Bay Frame 2	11.90	15.92	17.56	18.83	20.13	20.78	21.96
2-Bay Frame 3	9.32	12.31	13.18	13.75	14.25	14.48	14.85

For the non-interactive system, a constant modal damping ratio of 5% was adopted. Soil–structure interaction is provided by attaching frequency-independent springs (whose stiffness coefficients are those found in Ref. [12]) to the column bases in the different degrees of freedom. For simplicity, a modal damping ratio of 0.05 in all the modes was adopted for the interactive structure. To render the results of the interactive study realistic, the shear modulus of soil G_s has been varied from 10 to 500 MPa so that the results are representative of medium to hard soils where isolated footings are used to support light to medium structures. As a result, the time delay between excitation of extreme end footing varies from 0.0108 to 0.073 s for frames with one bay and 0.0208–0.147 s for frames with two bays. A value of 0.3 was adopted for the Poisson's ratio of soil, μ_s. A constant value of 1500 kg m^{-3} has been adopted to represent the mass density of soil over the entire G_s range.

The eigen values and eigen vectors of the undamped system necessary for computing the cross-correlation functions in Eq. (15) were obtained by the Jacobi method.

6. Results and discussion

Three loading conditions were considered:

(i) uniform horizontal base excitation (i.e. fully coherent excitations) is applied to the supports;
(ii) there is time delay in arrival of the horizontal excitation at successive supports (wave passage effect) as in Eqs. (7) and (8) which results in some degree of incoherence in the cross-spectral density functions of the support excitations; and
(iii) horizontal ground accelerations acting at different support are total independent due to a variety of factors like wave passage effect, wave reflections and refractions in the heterogeneous soil media and variations in local soil conditions at various supports.

An earlier study [9] has shown that for uniform base excitation (i.e. fully coherent excitations of the supports) the first mode of vibration yields a response which is lesser but over 99% of the response when all the modes are considered both for fixed base frames as well as frames with soil–structure interaction. In the current study, for the fixed base frames as well as when soil–structure interaction is considered, with multiple support excitations it was found that the fundamental mode yields in excess of 99% of the response obtained when all the modes are considered.

Table 1 presents the fundamental frequencies of the frames with soil–structure interaction. A fairly wide range of frequencies is covered by these structures so that many may not respond to the narrow band process generated by the Kanai filter parameters used in earlier studies [1,17] where the power density function of the ground acceleration is negligible for frequencies exceeding 30 rad/s.

As seen from Eq. (15) both the dynamic and pseudo-static displacements contribute to the root mean square (rms) value of the column shear. The wave passage effect can be quantified by a column shear ratio which is defined as the ratio of the rms value of the column shear (computed in terms of total displacements (Eq. (15)) in the end columns of the structure subjected to a time delay in the excitation of successive supports to the rms value of the column shear when the structure is subjected to uniform base excitation. The variation of this ratio with time delay is seen in Figs. 4 and 5 for 1-bay and 2-bay frames, respectively, in the absence of soil–structure interaction. The ratio is greater than 1.0 and found to monotonically increase with delay in the arrival of the excitation at successive supports for frames in the 2-bay configuration and for Frames 1 and 2 in the 1-bay configuration. The ratio increases marginally for Frame 3 of the 1-bay configuration. For this frame the highest value of the ratio is 1.0122 for a time delay of 0.03286 s. and it decreases to 1.004 for the largest time delay of 0.07348 s. The 2-bay configuration of any frame has a lower fundamental frequency compared to the 1-bay configuration (Table 1). Comparison of the column shear ratio obtained for any time delay between 1-bay and 2-bay configurations of any frame indicates that the wave passage effect is greater for the structure with greater number of supports, i.e., wave passage effect becomes more pronounced as the number of independently excitable structure supports increases.

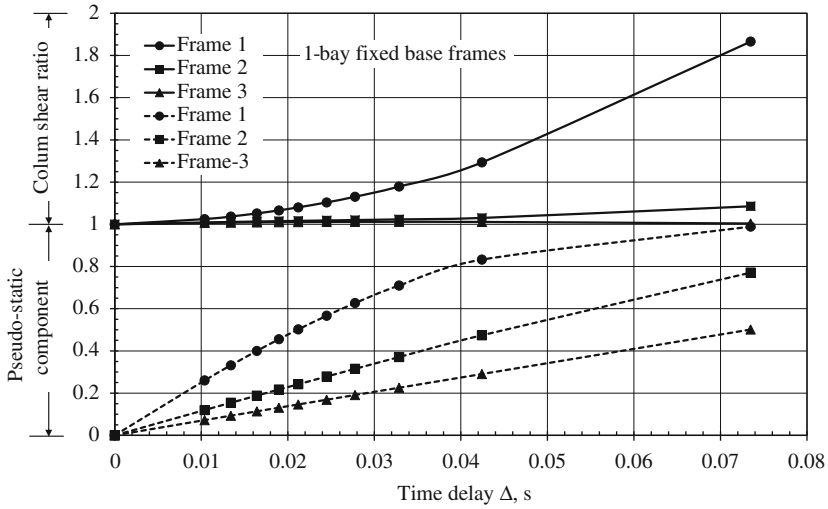

Fig. 4. Influence of wave passage effect on rms value of column shear and its pseudo-static displacement component for non-interactive 1-bay frames.

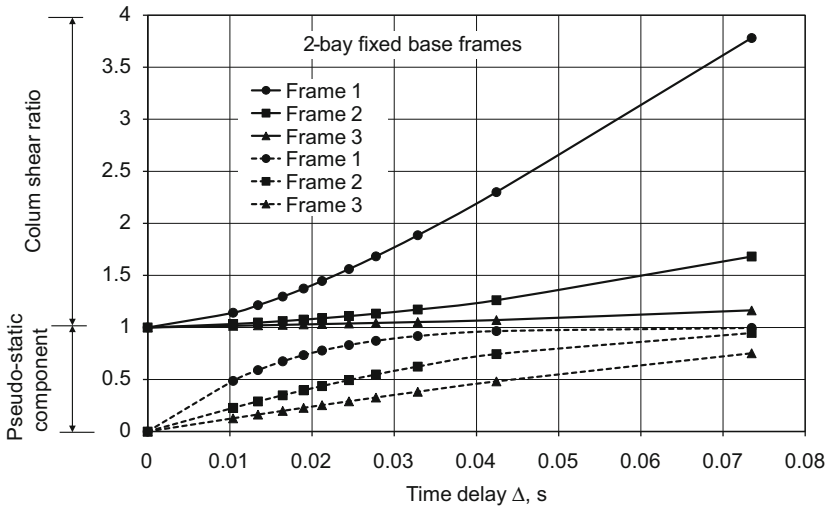

Fig. 5. Influence of wave passage effect on rms value of column shear and its pseudo-static displacement component for non-interactive 2-bay frames.

For Frame 3 in 1-bay and 2-bay configurations the wave passage effect in terms of changes in column shear ratio was either negligible or small (1.004 and 1.166, respectively) for the maximum delay of 0.07348 s. These frames also have the lowest natural frequencies (Table 1). To check the wave passage effect for very flexible frames, the elastic modulus for these two configurations of Frame 3 was reduced to one-tenth, so that their fundamental frequencies reduced to 5.382 and 4.070 rad/s, respectively. The rms value of the column shear with time delay was always greater than that obtained under uniform base excitation. The peak value of the column shear ratio was 1.0049 and occurred for a time delay of 0.04243 s. for the 1-bay configuration. The peak value of the column shear ratio for the 2-bay configuration was 1.011 and occurred for a time delay of 0.04243 s. This indicates that while wave passage effect increases the column shear in non-interactive frames, it is not of practical relevance in very flexible frames. The contribution of the pseudo-static displacements to the rms value of column shear for the analysis with wave passage effect is separable in Eqs. (A.3) and (A.4). The proportion the pseudo-static displacements contribution to the rms value of column shear for any time delay is also shown in Figs. 4 and 5 for the 1-bay and 2-bay non-interactive frames, respectively. It is seen that the pseudo-static contribution increases with time delay from zero (for no time delay) and can be as high as 99% (1-bay and 2-bay configurations of Frame 1) for the largest time delay of 0.07348 s. between successive supports (which corresponds to wave passage effect in soft soil with G_s=10 MPa).

It has been reported earlier [9] that for uniform support excitation, soil–structure interaction results in decrease in the rms value of column shear in extreme end columns with decrease in G_s for interactive frames subjected to a horizontal ground acceleration characterized by a white noise. In the current study the same effect of soil–structure interaction was

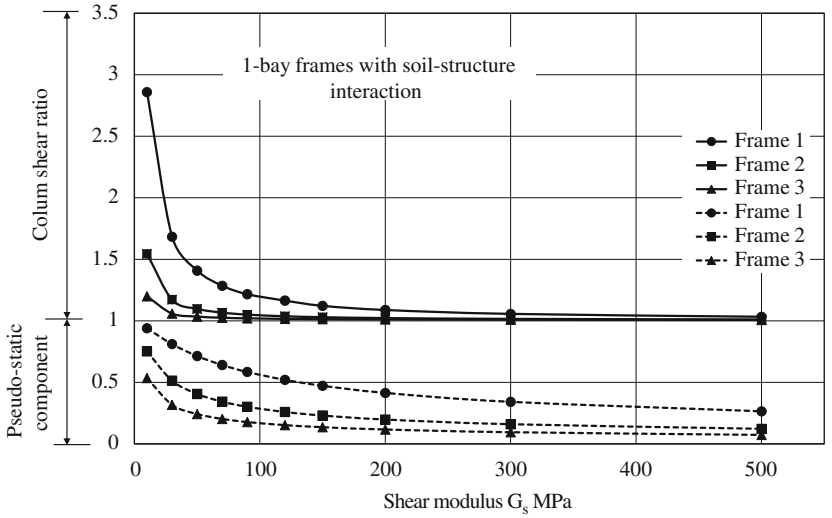

Fig. 6. Influence of soil–structure interaction on wave passage effect for 1-bay frames.

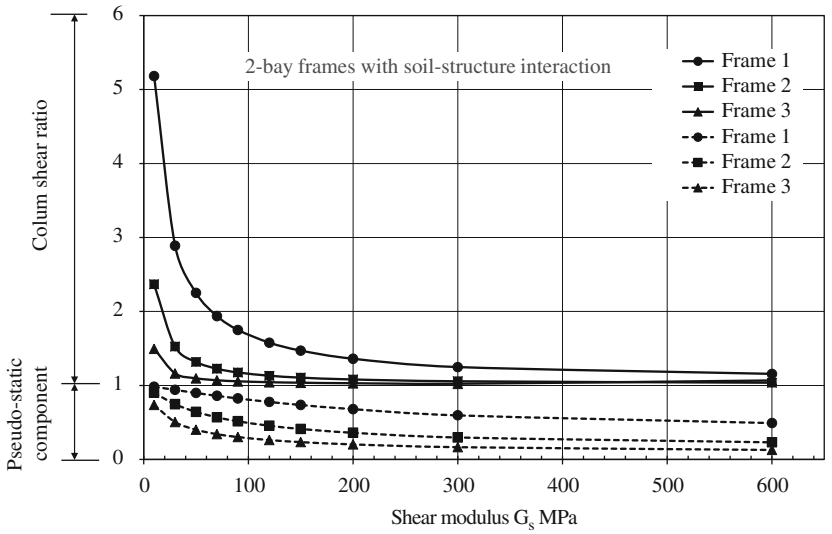

Fig. 7. Influence of soil–structure interaction on wave passage effect for 2-bay frames.

observed for the broad spectrum excitation used. The ratio of the RMS value of column shear in end columns of the interactive structure and the rms value of column shear in the non-interactive structure monotonically decreased from unity to 0.686, 0.722 and 0.784 as G_s decreased from infinity to 10 MPa in Frame 1, Frame 2 and Frame 3 in the 1-bay configuration. For the 2-bay configuration, the corresponding values of the column shear ratio were 0.739, 0.745 and 0.795 for Frame 1, Frame 2 and Frame 3, respectively.

The variation with respect to G_s of the soil of a column shear ratio (defined as the rms value of column shear in the interactive structure subjected to a time delay commensurate to the distance between supports and the G_s of the soil and the rms value of the column shear under uniform support excitation is shown in Fig. 6 for 1-bay frames and Fig. 7 for 2-bay frames. For all the frames in the 1-bay and 2-bay configurations, the ratio is greater than unity and increases with decrease in G_s over the entire G_s range investigated.

The wave passage effect on the rms value of column shear in extreme end columns is significant at low G_s (when the delay time is also larger). An examination of the rms value of column shear in extreme columns obtained for frames with soil–structure interaction subjected to wave passage effect and for corresponding fixed base frames subjected to a commensurate delay in arrival of the excitation at successive supports showed that the value differed by less than $\pm 5\%$.

Figs. 6 and 7 also indicate the pseudo-static component in the rms value of column shear of the structure subjected to wave passage effect. The pseudo-static component of the rms value of the column shear in the extreme columns decreases

with increase in G_s value. For low G_s values, where the time delay is large, the pseudo-static component (which is indicative of the wave passage effect) is large for a stiff interactive frame (94% and 98% for the 1-bay and 2-bay configurations of Frame 1, respectively) and *lesser* for flexible frames (53% and 74% for 1-bay and 2-bay configurations of Frame 3, respectively). For very stiff soils (G_s=500 MPa), the pseudo-static component of the rms value of column shear can be very low for a flexible frames (7% for 1-bay configuration of Frame 3).

The absolute value of the cross-spectral density functions, as discussed earlier, can decrease depending on the time delay and frequency. Soil heterogeneity at the supports is considered to bring in incoherence in the ground excitation. Differences in soil characteristics at the support can be accounted for in the soil impedance at each support. The assumption that the cross-spectral density functions are zero describes the situation where incoherence in the excitation at different supports arises due to spacing, frequency and modification the excitation undergoes during passage through the various strata.

For non-interactive frames, the ratio of the rms value of column shear arising due to non-coherent excitations at the support and the rms value of the column shear for the frame subjected to uniform support excitation is greater than

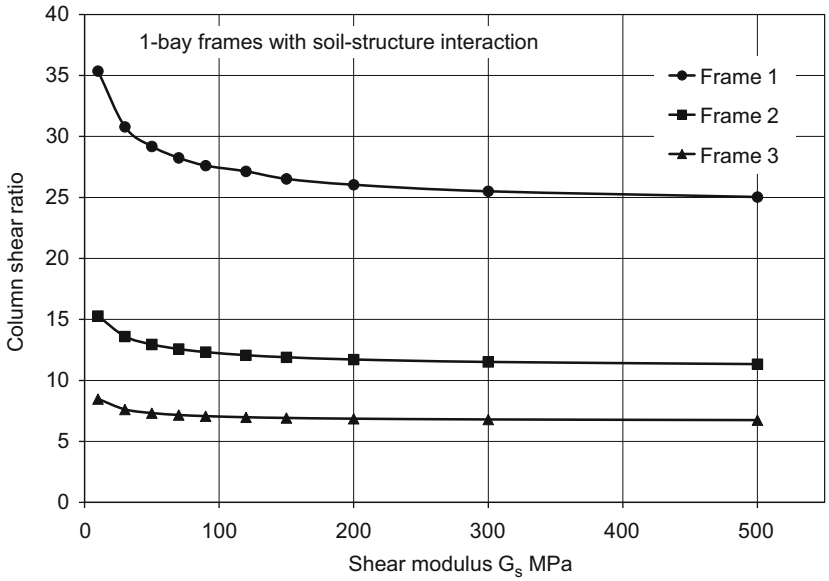

Fig. 8. Influence of soil–structure interaction on incoherency effect for 1-bay frames.

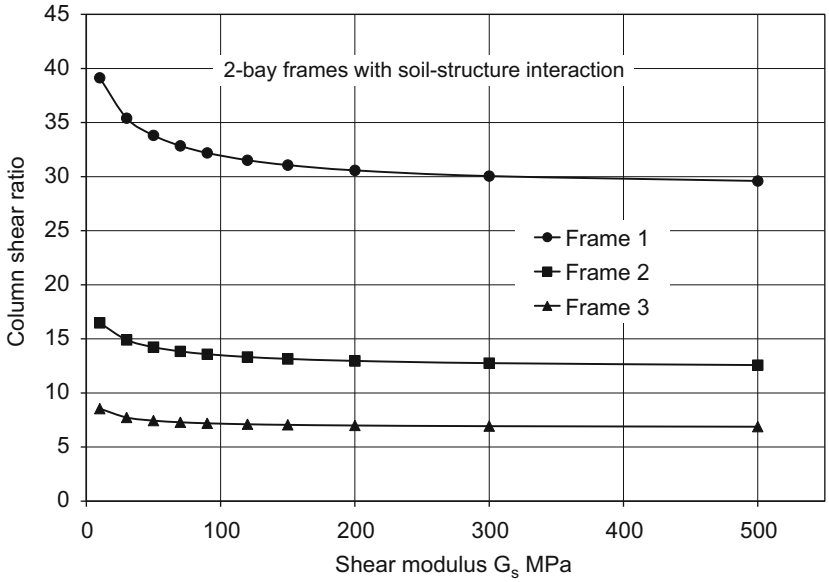

Fig. 9. Influence of soil–structure interaction on incoherency effect for 2-bay frames.

unity—around 24.3, 11 and 6.7 for the 1-bay frames in the descending order of their fundamental frequencies and 29, 12.3 and 6.8 for the 2-bay frames in the descending order of their fundamental frequencies. In all cases the pseudo-static component of the response was in excess of 99%.

When soil–structure interaction is accounted for, the ratio of the rms value of the column shear in extreme columns for uncorrelated excitation of supports to that for uniform support excitation was found to be influenced by the G_s value. The variation of this ratio with G_s is indicated in Figs. 8 and 9 for the 1-bay and 2-bay frames, respectively. The ratio decreases with increase in G_s and is higher for stiffer frames. For both 1-bay and 2-bay frames this ratio is seen to approach that for the corresponding non-interactive frame at very high values of G_s.

A study in the literature [10] on the response of a single-bay open-plane frame to multiple support horizontal seismic excitations has indicated that the response can differ significantly from that obtained for uniform base excitation. The findings are based on the response of a single frame with and without soil–structure interaction to five strong earthquake acceleration records.

To enhance understanding of the effect of multiple support excitations, the 3 frames of 2-bay configuration were subjected to the horizontal NS accelerogram of the El Centro 1940 earthquake. Details of this accelerogram are available in the literature [4,8,10]. It may be further added that the power spectral density (PSD) function this accelerogram has very strong peaks at frequencies of 14.57, 18.41 and 27.77 rad/s. An additional 7 significant peaks lie in the frequency range 21.9 and 26.6 rad/s.

Table 2
Peak shear developed in extreme columns of 2-bay fixed base frames subjected to multiple support excitation.

Delay (s)	0.0	0.01039	0.01342	0.01897	0.02121	0.02449	0.03286	0.07348
2-Bay Frame-1								
Peak column shear (kN)	71.898 (4.928)	112.440 (2.248)	124.800 (2.250)	149.110 (2.172)	160.500 (2.175)	176.280 (2.180)	213.770 (2.188)	366.460 (2.280)
Pseudo-static component (%)	0.0	36.52	47.16	68.77	71.76	76.03	82.81	≈ 100
2-Bay Frame-2								
Peak column shear (kN)	81.123 (2.583)	87.855 (2.590)	90.247 (2.453)	95.958 (2.458)	98.186 (2.460)	101.050 (2.462)	107.240 (2.470)	150.200 (2.225)
Pseudo-static component (%)	0.0	9.19	23.35	30.75	33.50	37.43	46.38	84.38
2-Bay Frame-3								
Peak column shear (kN)	68.845 (2.735)	71.877 (2.350)	73.224 (2.353)	75.274 (2.357)	76.175 (2.360)	77.152 (2.365)	79.442 (2.373)	99.463 (2.205)
Pseudo-static component (%)	0.0	8.07	10.28	13.97	15.60	17.75	23.18	55.08

The values in brackets denote the instant of excitation at which the peak response occurred.

Table 3
Peak shear developed in extreme columns of 2-bay frames subjected to multiple support excitation with soil–structure interaction.

	Shear modulus, G_s (MPa)						
	10	50	90	120	150	300	500
2-Bay Frame-1							
Peak column shear with no time delay (kN)	65.088 (4.728)	96.359 (2.550)	82.092 (2.520)	72.342 (2.513)	70.617 (2.510)	67.266 (2.680)	71.112 (2.263)
Peak column shear with time delay (kN)	383.930 (4.433)	227.140 (2.195)	171.170 (2.180)	143.290 (2.180)	129.760 (2.420)	110.510 (2.275)	107.630 (2.268)
P–S comp. (%)	93.65	79.76	78.22	82.42	63.51	45.77	36.91
2-Bay Frame-2							
Peak column shear with no time delay (kN)	100.750 (2.175)	71.786 (5.023)	71.742 (4.730)	71.410 (2.660)	74.777 (2.648)	79.460 (2.615)	79.579 (2.600)
Peak column shear with time delay (kN)	207.740 (2.240)	107.610 (4.857)	91.361 (4.370)	84.038 (2.190)	85.112 (2.343)	87.375 (4.515)	84.545 (2.458)
P–S comp. (%)	62.12	48.37	50.46	51.98	26.05	16.27	18.10
2-Bay Frame-3							
Peak column shear with no time delay (kN)	77.640 (2.250)	97.811 (2.160)	92.027 (5.107)	98.674 (5.088)	98.223 (5.075)	84.268 (5.048)	75.262 (5.040)
Peak column shear with time delay (kN)	114.510 (2.303)	123.650 (2.195)	102.790 (2.170)	99.069 (5.107)	99.093 (5.090)	86.552 (5.058)	77.376 (5.048)
P–S comp. (%)	45.92	24.45	20.39	2.98	3.08	3.93	3.64

The values in brackets denote the instant of excitation at which the peak response occurred.

Table 2 indicates the response of the 3 fixed base frames to uniform support excitation and also to multiple support excitations by this accelerogram. The frames possess 5% modal damping in all modes of excitation. The peak column increases with delay in arrival of the recorded ground accelerations at successive supports. This trend was also reported for a 1-bay open-plane frame with most of the accelerograms used in an earlier study [10]. The pseudo-static contribution to the peak column shear increases monotonically with delay. With a filtered white noise, the increase in column shear ratio with delay (wave passage effect) was not very significant for Frame 3 as seen in Fig. 5. This frame, however, responds strongly to delay with the selected accelerogram. For the maximum delay of 0.07348 s. the column shear is 1.55 times that obtained with uniform base excitation (Table 2). A major peak of the PSD function coincides with the fundamental natural frequency of this frame.

Table 3 presents the peak column shear developed in the 3 frames when soil–structure interaction is permitted. For uniform base excitation, Frame 1 has the highest peak column shear with G_s=50 MPa. In case of Frame 2, the peak value occurs with G_s=10 MPa, while for Frame 3 the peak value lies in the G_s range 120–150 MPa. In the literature [9] a decrease in the rms value of column shear with decrease in G_s has been reported when the excitation is a white noise and considering uniform base excitation.

With multiple support excitations under the selected accelerogram, the peak column shear value occurs for the Frames 1 and 2 at the lowest value of G_s (10 MPa) when the delay in arrival of the acceleration at successive supports is the maximum for the bay span selected (0.07348 s). The pseudo-static contribution to this peak column shear is also maximum for G_s=10 MPa. For Frame 3, the peak value occurs for G_s=50 MPa. It is also seen that the pseudo-static contribution is not the largest at the G_s where the peak column shear was maximum for this frame.

In general, the results in Tables 2 and 3 follow the trends observed with a filtered white noise.

7. Conclusions

(1) The effect of time delay (wave passage effect) on the response of some open-plane building frames on isolated footings subjected to a filtered white noise horizontal ground acceleration (broad spectrum process) can be significant even for the relatively short spans associated with such frames.
(2) It is seen that, in the absence of soil–structure interaction, increasing time delay increases the rms value of the column shear induced in extreme columns of the stiff frames. The wave passage effect is more severe for structures with larger number of supports. For more flexible frames it has little effect. In general, for larger time delays, it is observed in both stiff and relatively flexible frames that a significant proportion of the rms value of the column shear is contributed by the pseudo-static displacements arising from multiple support excitations.
(3) When soil–structure interaction is considered, the delay in arrival of the excitation at successive supports (which is larger for soils with low G_s values) does affect the rms value of the column shear in extreme end columns. The effect is significant at low G_s values and only for very stiff frames In general, wave passage effects are insignificant compared to the attenuating effect a decrease in G_s has on the response of an interactive structure to uniform support excitation. However, wave passage effects cause a significant proportion of the rms value of column shear to result from the induced pseudo-static displacements and the proportion ranges from 28% to 91% for low G_s to 7–44% for very high G_s—with stiffer frames more affected by these displacements.
(4) Increasing time delay or heterogeneity in soil conditions at different supports when interpreted as non-correlated excitations between individual supports has severe consequences for non-interactive frames subjected to horizontal ground acceleration. The rms values of columns shear under this condition are several times larger than those obtained for uniform support excitation. The very large contribution of pseudo-static displacements to the rms shear values ($>$ 99% even for the most flexible frame) suggest that a static analysis with properly chosen support displacements can substitute for a dynamic analysis for structural response to seismic multiple support excitations of framed structures.
(5) Soil–structure interaction has an attenuating effect (which decreases with increase in G_s) on the column shear ratio when support excitations are considered to be uncorrelated. Here too, the pseudo-static displacements contribute in excess of 98% to the rms column shear value. Further, even at very large G_s when the fundamental frequency is close to that of the non-interactive frame, the column shear ratio do not reach the value for the non-interactive frame because lateral support displacements are accompanied by significant displacements of the other elastically restrained support degrees of freedom.
(6) The responses of 2-bay frames to a strong motion accelerogram largely resemble those when a filtered white noise is used both for the fixed base condition and when soil–structure interaction is permitted.

Acknowledgments

The comments and suggestions of the reviewers have decidedly added to the worth of this study.

Appendix 1

Introducing total displacements in Eq. (13)

$$\text{shear}_{m_e} = [\mathbf{CSA}^{\mathrm{T}}]\{\mathbf{v}^t(\mathbf{t})_{m_e}\}/l_{m_e} \tag{A.1}$$

where $\{\mathbf{v}^{\mathbf{t}}(\mathbf{t})\} = \begin{Bmatrix} \mathbf{v}_s^d(\mathbf{t}) \\ \mathbf{v}_f^d(\mathbf{t}) \end{Bmatrix} + \begin{Bmatrix} \mathbf{v}_s^p(\mathbf{t}) \\ \{\mathbf{v}_g(\mathbf{t})\} \end{Bmatrix}$ and $\{\mathbf{v}_s^p(\mathbf{t})\} = [\overline{\mathbf{K}}]\{\mathbf{v}_g(\mathbf{t})\}$ and $\mathbf{v}_s^d(\mathbf{t}) = [\boldsymbol{\phi}]\{\mathbf{q}(\mathbf{t})\}$ as defined earlier in Section 2.

$$R_{\text{shear}_{m_e}}(\tau) = \frac{1}{l_{m_e}^2}[\mathbf{CSA}^{\mathrm{T}}][\mathbf{y}_m]\lim_{T\to\infty}\int_{-T/2}^{T/2}\{\mathbf{v}^t(\mathbf{t})\}\{\mathbf{v}^t(\mathbf{t}+\boldsymbol{\tau})\}^{\mathrm{T}}\,\mathrm{d}\mathbf{t}[\mathbf{y}_m]^{\mathrm{T}}[\mathbf{CSA}^{\mathrm{T}}]^{\mathrm{T}} \tag{A.2}$$

or

$$R_{\text{shear}_{m_e}}(\tau) = \frac{1}{l_{m_e}^2}[\mathbf{CSA}^{\mathrm{T}}][\mathbf{y}_m][\mathbf{R}_{v^t}(\tau)][\mathbf{y}_m]^{\mathrm{T}}[\mathbf{CSA}^{\mathrm{T}}]^{\mathrm{T}} \tag{A.3}$$

It can be shown that

$$[\mathbf{R}_{v^t}(\boldsymbol{\tau})] = \begin{bmatrix} \mathbf{R}_{v^t 11}(\boldsymbol{\tau}) & \mathbf{R}_{v^t 12}(\boldsymbol{\tau}) \\ \mathbf{R}_{v^t 21}(\boldsymbol{\tau}) & \mathbf{R}_{v^t 22}(\boldsymbol{\tau}) \end{bmatrix} \tag{A.4}$$

where

$$[\mathbf{R}_{v^t 11}(\boldsymbol{\tau})] = [\mathbf{R}_{v^{dd}}(\boldsymbol{\tau})] + [\mathbf{R}_{v^{dp}}(\boldsymbol{\tau})] + [\mathbf{R}_{v^{pd}}(\boldsymbol{\tau})] + [\mathbf{R}_{v^{pp}}(\boldsymbol{\tau})] \tag{A.4a}$$

$$[\mathbf{R}_{v^t 12}(\boldsymbol{\tau})] = [\mathbf{R}_{v^{dg}}(\boldsymbol{\tau})] + [\mathbf{R}_{v^{pg}}(\boldsymbol{\tau})] \tag{A.4b}$$

$$[\mathbf{R}_{v^t 21}(\boldsymbol{\tau})] = [\mathbf{R}_{v^{gd}}(\boldsymbol{\tau})] + [\mathbf{R}_{v^{gp}}(\boldsymbol{\tau})] \tag{A.4c}$$

and

$$[\mathbf{R}_{v^t 22}(\boldsymbol{\tau})] = [\mathbf{R}_{v^g}(\boldsymbol{\tau})] \tag{A.4d}$$

where the superscripts d, g and p represent the dynamic displacements, specified support motions and motions induced at other degrees of freedom by these specified support motions ($\mathbf{v}^g$), respectively

$$[\mathbf{R}_{v_{rs}^{dd}}(\mathbf{0})] = \frac{1}{2\pi}\{\boldsymbol{\phi}_r\}[\mathbf{m}]\begin{bmatrix}\overline{\mathbf{K}} \\ \mathbf{I}\end{bmatrix}\left[\int_{-\infty}^{\infty} G_r^*(\boldsymbol{\omega})G_s(\boldsymbol{\omega})\mathbf{S}_{\ddot{v}_{g_{ij}}}(\boldsymbol{\omega})\,\mathrm{d}\omega\right]\begin{bmatrix}\overline{\mathbf{K}} \\ \mathbf{I}\end{bmatrix}^{\mathrm{T}}[\mathbf{m}]^{\mathrm{T}}\{\boldsymbol{\phi}_s\} \tag{A.5a}$$

$$[\mathbf{R}_{v_{rs}^{dp}}(\mathbf{0})] = -\frac{1}{2\pi}[\boldsymbol{\phi}][\mathbf{A}_{ri}]\left[\int_{-\infty}^{\infty}\frac{G_r^*(\boldsymbol{\omega})\mathbf{S}_{\ddot{v}_{g_{ij}}}(\boldsymbol{\omega})}{\omega^2}\,\mathrm{d}\boldsymbol{\omega}\right][\overline{\mathbf{K}}_{js}^{\mathrm{T}}] \tag{A.5b}$$

$$[\mathbf{R}_{v_{rs}^{pd}}(\mathbf{0})] = -\frac{1}{2\pi}[\overline{\mathbf{K}}_{ri}]\left[\int_{-\infty}^{\infty}\frac{\mathbf{S}_{\ddot{v}_{g_{ij}}}(\boldsymbol{\omega})G_s(\boldsymbol{\omega})}{\omega^2}\,\mathrm{d}\boldsymbol{\omega}\right][\mathbf{A}_{js}][\boldsymbol{\phi}_s^{\mathrm{T}}] \tag{A.5c}$$

$$[\mathbf{R}_{v_{ij}^{pp}}(\mathbf{0})] = \frac{1}{2\pi}[\overline{\mathbf{K}}_i]\left[\int_{-\infty}^{\infty}\frac{\mathbf{S}_{\ddot{v}_{g_{ij}}}(\boldsymbol{\omega})}{\boldsymbol{\omega}^4}\,\mathrm{d}\boldsymbol{\omega}\right][\overline{\mathbf{K}}_j^{\mathrm{T}}] \tag{A.5d}$$

$$[\mathbf{R}_{v_{rj}^{dg}}(\mathbf{0})] = -\frac{1}{2\pi}[\boldsymbol{\phi}][\mathbf{A}_{ri}]\left[\int_{-\infty}^{\infty}\frac{G_r^*(\boldsymbol{\omega})\mathbf{S}_{\ddot{v}_{g_{ij}}}(\boldsymbol{\omega})}{\omega^2}\,\mathrm{d}\boldsymbol{\omega}\right] \tag{A.5e}$$

$$[\mathbf{R}_{v_{is}^{gd}}(\mathbf{0})] = \frac{1}{2\pi}\left[\int_{-\infty}^{\infty}\frac{\mathbf{S}_{\ddot{v}_{g_{ij}}}G_s(\boldsymbol{\omega})}{\omega^2}\,\mathrm{d}\boldsymbol{\omega}\right][\mathbf{A}_{js}^{\mathrm{T}}][\boldsymbol{\phi}_s^{\mathrm{T}}] \tag{A.5f}$$

$$[\mathbf{R}_{v_{ij}^{gp}}(\mathbf{0})] = \frac{1}{2\pi}\left[\int_{-\infty}^{\infty}\frac{\mathbf{S}_{\ddot{v}_{g_{ij}}}(\boldsymbol{\omega})}{\boldsymbol{\omega}^4}\,\mathrm{d}\boldsymbol{\omega}\right][\overline{\mathbf{K}}_j^{\mathrm{T}}] \tag{A.5g}$$

$$[\mathbf{R}_{v_{ij}^{pg}}(\mathbf{0})] = = \frac{1}{2\pi}[\overline{\mathbf{K}}_i]\left[\int_{-\infty}^{\infty}\frac{\mathbf{S}_{\ddot{v}_{g_{ij}}}(\boldsymbol{\omega})}{\boldsymbol{\omega}^4}\,\mathrm{d}\boldsymbol{\omega}\right] \tag{A.5h}$$

$$[\mathbf{R}_{v^g}(\mathbf{0})] = \frac{1}{2\pi}\left[\int_{-\infty}^{\infty}\frac{\mathbf{S}_{\ddot{v}_{g_{ij}}}(\boldsymbol{\omega})}{\boldsymbol{\omega}^4}\,\mathrm{d}\boldsymbol{\omega}\right] \tag{A.5i}$$

References

[1] A.D. Kiureghian, A. Neuenhofer, Response spectrum method for multi-support seismic excitations, *Earthquake Engineering and Structural Dynamics* 21 (1992) 713–740.
[2] A.D. Kiureghian, A coherency model for spatially varying ground motions, *Earthquake Engineering and Structural Dynamics* 25 (1996) 99–111.
[3] J.L. Bogdanoff, J.E. Goldberg, A.J. Schiff, The effect of ground transmission time on the response of long structures, *Bulletin of the Seismological Society of America* 55 (1965) 627–640.
[4] R.H. Clough, J. Penzien, *Dynamics of Structures*, first ed, McGraw-Hill, New York, 1975.
[5] R.A. Parmelee, Building–foundation interaction effects, *Journal of the Engineering Mechanics Division, American Society of Civil Engineers* 93 (1967) 131–152.
[6] J.H. Rainer, Structure–ground interaction in earthquakes, *Journal of the Engineering Mechanics Division, American Society of Civil Engineers* 97 (1971) 1431–1450.
[7] P.C. Jennings, J. Bielak, Dynamics of building–soil interaction, *Bulletin of the Seismological Society of America* 63 (1973) 9–48.
[8] K.V. Rambabu, M.M. Allam, Adequacy of the Parmelee model to represent open plane frames on isolated footings under seismic excitation, *Journal of Sound and Vibration* 258 (2002) 969–980.
[9] S.M. Basha, M.M. Allam, Response of open-plane frames on isolated footings to an excitation characterized by a white noise, *Journal of Sound and Vibration* 275 (2004) 1085–1100.
[10] K.V. Rambabu, M.M. Allam, Response of an open-plane frame to multiple support horizontal seismic excitations with soil–structure interaction, *Journal of Sound and Vibration* 299 (2007) 388–396.
[11] A. Zerva, H.-S. Ang, Y.K. Wen, Lifeline response to spatially variable ground motions, *Earthquake Engineering and Structural Dynamics* 16 (1988) 361–379.
[12] A. Pais, E. Kausel, Approximate formulas for dynamic stiffness of rigid foundations, *Soil Dynamics and Earthquake Engineering* 7 (1988) 213–227.
[13] M. Novak, L. El Hifnaway, Effect of soil–structure interaction on damping of structures, *Earthquake Engineering and Structural Dynamics* 11 (1983) 595–621.
[14] N.C. Tsai, D. Neihoff, M. Swatta, A.H. Hadjian, The use of frequency-independent soil–structure interaction parameters, *Nuclear Engineering and Design* 31 (1974) 168–183.
[15] M.A. Sarrazin, J.M. Rosset, R.V. Whitman, Dynamic soil–structure interaction, *Journal of the Structural Division, American Society of Civil Engineers* 98 (1972) 1525–1544.
[16] J.M. Rosset, R.V. Whiteman, R. Dobry, Modal analysis for structures with foundation interaction, *Journal of Structural Division, American Society of Civil Engineers* 99 (1973) 399–416.
[17] A. Zerva, Response of multi-span beams to spatially incoherent seismic ground motions, *Earthquake Engineering and Structural Dynamics* 19 (1990) 819–832.